A Multinuclear ENDOR Study of the C-Cluster in CO Dehydrogenase from *Clostridium thermoaceticum*: Evidence for H_xO and Histidine Coordination to the $[Fe_4S_4]$ Center

Victoria J. DeRose,*,† Joshua Telser,‡,§ Mark E. Anderson,† Paul A. Lindahl,*,† and Brian M. Hoffman*,‡

Contribution from the Departments of Chemistry, Texas A&M University, College Station, Texas 77842-3012, and Northwestern University, Evanston, Illinois 60208-3113

Received September 8, 1997

Abstract: The C-cluster of carbon monoxide dehydrogenase (CODH) catalyzes the reversible oxidation of CO to form CO_2. This study reports electron nuclear double resonance (ENDOR) spectroscopy of the one-electron reduced (C_{red1}), the CN^--inhibited, and the CO (or dithionite)-reduced (C_{red2}) forms of the C-cluster from *Clostridium thermoaceticum* CODH ($CODH_{Ct}$). The observed hyperfine interactions of $^{1,2}H$, ^{14}N, ^{13}C, and ^{57}Fe support and extend the current Ni−X−$[Fe_4S_4]$ C-cluster model in which a $[Fe_4S_4]$ center is linked to a Ni ion through a unique iron, FCII. The unpaired electron spin apparently is localized on the $[Fe_4S_4]$ component of the cluster, and thus the hyperfine interactions observed by ENDOR most probably reflect species associated with that component. A solvent-exchangeable proton with a maximum hyperfine coupling of $A(^1H) = 16$ MHz is detected in the C_{red1} form, but not in the CN^--inhibited or C_{red2} forms. The exchangeable proton is assigned to a probable solvent-derived (H_xO, $x = 1, 2$) ligand to FCII of the C_{red1} $[Fe_4S_4]^{1+}$ center and is predicted to be a substrate in CO/CO_2 catalysis. For both C_{red1} and C_{red2}, we find ENDOR features in the region expected for a nitrogen-donor ligand which likely arise from a histidine ligand to the $[Fe_4S_4]$ center. ^{57}Fe ENDOR detects at least two classes of Fe in C_{red1} that most likely arise from the $(Fe^{2.5+})_2$ mixed-valence pair. Their large maximum couplings of $A(^{57}Fe) > 40$ MHz support the unusual nature of the cluster; these do not change dramatically between the C_{red1} and C_{red2} forms of the enzyme. C_{red2} formed by reduction with ^{13}CO reveals no new ^{13}C features, strongly suggesting that neither CO nor its oxidized products are bound to the $[Fe_4S_4]$ center in C_{red2}. Taken together, these ENDOR assignments suggest that in the C_{red1} state, the unique Fe ion of the CODH C-cluster has an available coordination site that stably binds H_xO or CN^- and that reduction of the C-cluster results in rearrangement at that site, causing loss of the bound aqueous ligand.

Introduction

In certain acetogenic, methanogenic, and photosynthetic bacteria, an oxygen-sensitive Ni-containing enzyme known as carbon monoxide dehydrogenase (CODH)[1] catalyzes the reversible oxidation of CO to CO_2 (eq 1).

$$CO + OH^- = CO_2 + H^+ + 2e^- \quad (1)$$

Ni-containing CODH's constitute one of only five known classes of Ni enzymes, and the structures of the metal centers and in particular the involvement of Ni in catalysis remain under investigation. CODH from photosynthetic *Rhodospirillum rubrum* ($CODH_{Rr}$) is a monomer (62 kDa) that catalyzes only CO/CO_2 redox chemistry,[2,3] whereas the enzyme from the acetogen *Clostridium thermoaceticum* ($CODH_{Ct}$) is an $\alpha_2\beta_2$ tetramer (310 kDa) that in addition catalyzes the synthesis of acetyl-CoA.[4] Certain methanogens (e.g., *Methanothrix soehngenii*) contain a multimeric CODH ($CODH_{Ms}$) that also participates in the synthesis of methane from acetyl-CoA.[4] Current spectroscopic and genetic evidence indicates that all known Ni-containing CODH's use essentially the same two metal clusters for CO/CO_2 redox catalysis: a novel Ni−$[Fe_4S_4]$ center known as the *C-cluster* and a standard $[Fe_4S_4]^{2+/1+}$ cluster called the *B-cluster*.[5,6] The C-cluster is the active site for CO/CO_2 redox chemistry,[7−9] and the B-cluster functions to transfer electrons between the C-cluster and external redox agents.[6,9] In $CODH_{Ct}$, a third cluster, the *A-cluster*, is involved in acetyl-CoA synthesis.

§ Permanent address: Chemistry Program, Roosevelt University, 430 S. Michigan Ave., Chicago, IL 60605-1394.

† Texas A&M University.

‡ Northwestern University.

(1) Abbreviations: CODH, carbon monoxide dehydrogenase; $CODH_{Ct}$, CODH from *C. thermoaceticum*; $CODH_{Rr}$, CODH from *R. rubrum*; $CODH_{Ms}$, CODH from *M. soehngenii*; C_{red1}, 1-electron reduced form of the C-cluster; C_{red2}, CO (or dithionite)-reduced C-cluster; B_{red}, reduced form of CODH B-cluster; ENDOR, electron nuclear double resonance; ESEEM, electron spin−echo envelope modulation; CW, continuous wave; H_s, strongly coupled proton(s); H_m, moderately coupled proton(s); rf, radio frequency; fwhm, full-width at half-maximum height.

(2) Bonam, D.; Ludden, P. W. *J. Biol. Chem.* **1987**, *262*, 2980−2987.
(3) Kerby, R. L.; Hong, S. S.; Ensign, S. A.; Coppoc, L. J.; Ludden, P. W.; Roberts, G. P. *J. Bacteriol.* **1992**, *174*, 5284−5294.
(4) Ragsdale, S. W.; Kumar, M. *Chem. Rev.* **1996**, *96*, 2515−2539.
(5) Hu, Z.; Spangler, N. J.; Anderson, M. E.; Xia, J.; Ludden, P. W.; Lindahl, P. A.; Münck, E. *J. Am. Chem. Soc.* **1996**, *118*, 830−845.
(6) Anderson, M. E.; Lindahl, P. A. *Biochemistry* **1994**, *33*, 8702−8711.
(7) Anderson, M. E.; DeRose, V. J.; Hoffman, B. M.; Lindahl, P. A. *J. Inorg. Biochem.* **1993**, *51*, Abstract B149.
(8) Anderson, M. A.; DeRose, V. J.; Hoffman, B. M.; Lindahl, P. A. *J. Am. Chem. Soc.* **1993**, *115*, 12204−12205.
(9) Kumar, M.; Lu, W.-P.; Liu, L.; Ragsdale, S. W. *J. Am. Chem. Soc.* **1993**, *115*, 11646−11647.

S0002-7863(97)03148-X CCC: $15.00
Published on Web 08/18/1998

Table 1. Properties of the B- and C-Clusters of $CODH_{Ct}$

$cluster_{state}$	C_{ox}	C_{red1}	C_{red2}	C_{red1} (CN^-)	B_{red}
reduction potential		-220 $mV^{ox/red1}$	-530 $mV^{red1/red2}$		-440 $mV^{ox/red}$
spin state *S* (ground)	0	$^1/_2$	$^1/_2$	$^1/_2$	$^1/_2$
EPR signal	(EPR silent)	[2.01, 1.81, 1.65];	[1.97, 1.87, 1.75];	[1.87, 1.78, 1.55];	[2.04, 1.94, 1.90];
$[g_1, g_2, g_3]$		$g_{av} = 1.82$	$g_{av} = 1.86$	$g_{av} = 1.72$	$g_{av} = 1.96$
proposed oxidation states	L_{ox}:Ni^{2+}:$[Fe_4S_4]^{2+}$	L_{ox}:Ni^{2+}:$[Fe_4S_4]^{+}$	L_{red}:Ni^{1+}:$[Fe_4S_4]^{+}$	L_{ox}:Ni^{2+}:$[Fe_4S_4]^{+}$-CN^-	$[Fe_4S_4]^{1+}$

The CODH C-cluster is stable in three oxidation states, denoted C_{ox}, C_{red1}, and C_{red2}, whose properties for $CODH_{Ct}$ are summarized in Table 1. Reduction of the diamagnetic C_{ox} state by one electron forms C_{red1}, an $S = {}^1/_2$ state yielding (for $CODH_{Ct}$) an EPR signal with $g_{av} = 1.82$. Further reduction of the C-cluster affords C_{red2}, which also has an $S = {}^1/_2$ EPR signal, but one that is slightly altered from that of C_{red1}. Binding of small anions such as CN^- also affect the C-cluster EPR signal.

The C-cluster has unusual EPR, redox, and Mössbauer properties that are best described as arising from a Ni−X−$[Fe_4S_4]$ cluster wherein a unique Fe of the $[Fe_4S_4]$ center is linked to the Ni ion through one or more bridging ligands (X).[5,10] Mössbauer properties of the unique Fe, which is known as FCII (ferrous component II), indicate a 5- or 6-coordinate site.[5,13] Exogenous ligands of the cluster, including the ligands to FCII and the bridging ligand(s), have not yet been identified.

Evidence that the Ni is bridged to the $[Fe_4S_4]$ center is indirect, but substantial. CODH from *R. rubrum* can be isolated in an inactive Ni-deficient form that is reactivated by incubation in aqueous Ni(II).[14] The Ni-deficient C-cluster contains an Fe_4S_4 center with altered EPR, redox, and Mössbauer properties. Ni incubation causes the spectroscopic signatures of the unique FCII iron to appear,[5] and the C-cluster $E°$ to increase by ~0.2 V.[15] The simplest explanation for these results for $CODH_{Rr}$ is that Ni binds near to the Fe_4S_4 center and organizes a bridge to the iron that becomes FCII, and that this arrangement increases the redox potential of the Fe_4S_4 center.

Mössbauer[5,16,17] and EXAFS[18] spectroscopies have established metal oxidation states of Ni^{2+}−X−$[Fe_4S_4]^{1+}$ for C_{red1}. Hu et al.[5] have proposed that the C_{red1} EPR signal arises predominantly from the $S = {}^1/_2$ $[Fe_4S_4]^{1+}$ component of the C-cluster and that the Ni^{2+} is at most weakly coupled to the electron spin. C_{red2} is formed by reducing C_{red1} with two-electron reductants such as substrate CO or dithionite, and so C_{red2} appears to be two electrons more reduced than C_{red1}. Assigning oxidation states for C_{red2} is problematic, however, because this state also appears to include a $[Fe_4S_4]^{1+}$ cluster,[5] and Ni^0 has not been observed in any biomolecule. Anderson and Lindahl[19] have proposed a scheme for the C_{red1} to C_{red2} conversion in which an unidentified redox-active ligand, L, and Ni^{2+} each undergo a one-electron reduction.[20]

The oxidation of CO likely involves the nucleophilic attack of a metal-bound CO by water or hydroxide (H_xO). The current Ni−X−$[Fe_4S_4]$ C-cluster model forms the basis of a proposed "bimetallic" catalytic mechanism, wherein the reactants are bound at the bridged Ni and Fe sites. From the EPR, redox, and catalytic properties of the C-cluster, Anderson and Lindahl[6] proposed that CO binds to the C-cluster in its C_{red1} state and that C_{red2} is generated as CO is oxidized to CO_2. A pH dependence of k_{cat}/K_m plus small pH-dependent shifts in the C_{red1} EPR signal led Seravelli et al.[21] to propose that a metal-bound water with a $pK_a = 7.2$ participates in catalysis. Hu et al.[5] have suggested that, during CO oxidation, CO binds to the Ni center and OH^- to FCII.

The structure of the C-cluster has been probed by examining the effects of small anions and CO/CO_2 analogues such as N_3^-, SCN^-, and CN^-, all of which perturb the C-cluster.[6,8,21,22] The best-characterized of these, cyanide, inhibits the CO oxidation reaction and binds to the $[Fe_4S_4]^{1+}$ cluster[8] at FCII.[5] Azide binds to the C-cluster at an unknown site, and its effect on the C-cluster EPR signal is dramatically different from that of CN^-, causing a shift to $g_{av} > 2$ from $g_{av} = 1.82$ for C_{red1} and $g_{av} = 1.72$ for $C_{red1}(CN^-)$. Hu et al.[5] suggested that the effect of small molecules on the C-cluster EPR signal was due to perturbation of the weak exchange coupling between the $[Fe_4S_4]$ center and the Ni ion.

Electron nuclear double resonance (ENDOR) and electron spin−echo envelope modulation (ESEEM) spectroscopic techniques detect nuclei coupled to the electron spin of a paramagnetic cluster. These techniques are important in identifying metal centers and ligands associated with EPR-active metal clusters in proteins and have been used to identify all atoms associated with Fe−S clusters, including small molecule ligands

(10) The C-cluster also has been investigated by resonance Raman spectroscopy (ref 11), but these papers recently have been retracted (ref 12) and so are not discussed here.

(11) (a) Qiu, D.; Kumar, M.; Ragsdale, S. W.; Spiro, T. G. *J. Am. Chem. Soc.* **1995**, *117*, 2653−2654. (b) Qiu, D.; Kumar, M.; Ragsdale, S. W.; Spiro, T. G. *J. Am. Chem. Soc.* **1996**, *118*, 10429−10435.

(12) *J. Am. Chem. Soc.* **1997**, *119*, 11134.

(13) (a) The most fully characterized $[Fe_4S_4]$ center with a unique Fe is that of beef heart aconitase (ref 13b). In the absence of substrate, Fe_a of aconitase is coordinated by three bridging sulfides and one terminal hydroxyl ligand. In the presence of substrate, Fe_a is six-coordinate with two oxygen ligands from *trans*-aconitate, one aqueous ligand, and the bridging sulfides. The Mössbauer parameters of FCII in $CODH_{Rr}$ are intermediate between those of substrate-free and substrate-bound aconitase (ref 5), but are quite similar to a five-coordinate mononuclear Fe model complex that has S_3N_2 coordination (ref 13c). For this reason it has been proposed that the unique Fe in the CODH C-cluster is five-coordinate in the C_{red1} state. (b) Beinert, H.; Kennedy, M. C.; Stout, C. D. *Chem. Rev.* **1996**, *96*, 2335−2373. (c) Ciurli, S.; Carrié, M.; Weigel, J. A.; Carney, M. J.; Stack, T. D. P.; Papaefthymiou, G. C.; Holm, R. H. *J. Am. Chem. Soc.* **1990**, *112*, 2654−2664.

(14) (a) Ensign, S. A.; Bonam, D.; Ludden, P. W. *Biochemistry* **1989**, *28*, 4968−4973. (b) Ensign, S. A.; Campbell, M. J.; Ludden, P. W. *Biochemistry* **1990**, *29*, 2162−2168.

(15) Spangler, N. J.; Lindahl, P. A.; Bandarian, V.; Ludden, P. W. *J. Biol. Chem.* **1996**, *271*, 7973−7977.

(16) Lindahl, P. A.; Ragsdale, S. W.; Münck, E. *J. Biol. Chem.* **1990**, *265*, 3880−3888.

(17) Lindahl, P. A.; Münck, E.; Ragsdale, S. W. *J. Biol. Chem.* **1990**, *265*, 3873−3879.

(18) Tan, G. O.; Ensign, S. A.; Ciurli, S.; Scott, M. J.; Hedman, B.; Holm, R. H.; Ludden, P. W.; Korszun, Z. R.; Stephens, P. J.; Hodgson, K. O. *Proc. Natl. Acad. Sci. U.S.A.* **1992**, *89*, 4427−4431.

(19) Anderson, M. E.; Lindahl, P. A. *Biochemistry* **1996**, *35*, 8371−8380.

(20) Our use in Table 1 of the redox active ligand L is for electron-bookkeeping purposes only. At present, there is no independent evidence either for such a ligand or a Ni oxidation state change in C_{red2}. An alternative model is that in the C_{red1} to C_{red2} conversion, a separate, unidentified species becomes reduced instead of the C-cluster. This model would leave the C-cluster isoelectronic in the two states, but involves the complication of an additional, unidentified redox-active species (with $E_m' = -530$ mV) and so was rejected by Anderson and Lindahl (ref 19).

(21) Seravalli, J.; Kumar, M.; Lu, W.-P.; Ragsdale, S. W. *Biochemistry* **1995**, *34*, 7879−7888.

(22) Kumar, M.; Lu, W.-P.; Smith, A.; Ragsdale, S. W.; McCracken, J. *J. Am. Chem. Soc.* **1995**, *117*, 2939−2944.

and protons involved in hydrogen bonds.[23−26] A thorough ENDOR investigation has been performed of the $CODH_{Ct}$ A-cluster,[27] which is responsible for synthesis of acetyl-CoA. The A-cluster also is a Ni−$[Fe_4S_4]$ center, and it is EPR-active upon reduction with CO. Unlike the native C-cluster, however, the CO-reduced A-cluster gives rise to an EPR signal with $g_{av} > 2$, indicating that spin coupling in the two clusters is different. For the A-cluster, analysis of hyperfine couplings to ^{61}Ni and ^{57}Fe of the metal center and to ^{13}C from bound ^{13}CO aided in identifying the components of that center.[27]

ENDOR and ESEEM have been selectively employed to discern binding of isotopically labeled CN^- and N_3^- to the $CODH_{Ct}$ C-cluster,[7,8,22] but a more complete study of the C-cluster itself has been lacking. Here, we report the results of ^{1,2}H, ^{13}C, ^{14}N, ^{57}Fe, and ^{61}Ni ENDOR spectroscopy for the $CODH_{Ct}$ C-cluster in the C_{red1}, C_{red2}, and CN^--perturbed forms. In this study, evidence is reported for a strongly coupled, solvent-exchangeable proton from a ligand that is bound in the C_{red1} state but not the C_{red2} state. This proton is suggested to arise from a water or hydroxide (H_xO) ligand that is bound to FCII of the $[Fe_4S_4]$ cluster and that attacks metal-bound CO during catalysis. The ENDOR results also provide evidence for a putative histidine ligand along with cysteine ligands to the $[Fe_4S_4]$ component of the C-cluster. We examine the effects of CN^- binding and the electronic changes associated with the C_{red1}/C_{red2} conversion.

Materials and Methods

Bacterial Growth and Purification of $CODH_{Ct}$. *Clostridium thermoaceticum* cells were grown and $CODH_{Ct}$ was purified and characterized as described.[28,29] For isotopically labeled $CODH_{Ct}$, the yeast-extract/tryptone solution was passed through a Chelex (BioRad) column, glassware was soaked in dilute acid prior to use, and the medium was enriched in ^{57}Fe (10 mg/17 L carboy) or ^{61}Ni (4 mg/17 L carboy). CO oxidation activities ranged from 240 to 409 units/mg and CO/acetyl-CoA exchange activities from 0.06 to 0.19 units/mg. Potassium cyanide (Baker) was prepared in 50 mM NaOH. Sodium dithionite ($Na_2S_2O_4$) and thionin (3,7-diaminophenothiazin-5-ium chloride) were purchased from Aldrich and standardized as described.[6] Protein concentrations were determined by the Biuret method[30] using bovine serum albumin (Sigma) as a standard. A molecular weight of 154.7 kDa for each $CODH_{Ct}$ dimer was used in calculations. All manipulations of $CODH_{Ct}$ were performed anaerobically either in an argon-atmosphere glovebox (Vacuum/Atmospheres, model HE-453; Teledyne 310 analyzer; 0.5−1 ppm O_2) or on a CO Schlenk manifold. Samples were desalted and made free of dithionite by passage through a Sephadex G-25 column equilibrated in Tris-HCl pH 8.0. H_2O in $CODH_{Ct}$ samples was replaced with D_2O in one of two ways. In one method, samples were chromatographed through a G-25 column equilibrated in D_2O and 50 mM Tris-DCl pD 8.0 (read 7.6 on the pH meter).[31] In the other method, H_2O-containing samples were concentrated using a Centricon unit (Amicon) and diluted with D_2O-containing buffer a sufficient number of times to achieve >90% final D_2O content. All D_2O samples were allowed to exchange for 15−36 h before concentration and manipulation.

Electron Nuclear Double Resonance Spectroscopy. Continuous wave (CW) Q-band (35 GHz) ENDOR spectra were collected at 2 K as described[23,24,32,33] by using 100 kHz magnetic field modulation; the rf is not modulated, but a broadened rf band width (200 kHz) was used in some cases to improve signal-to-noise for broad ENDOR lines.[34] The ENDOR transitions observed in this manner approximate the absorptive line shapes, commonly with some distortion such as a higher apparent intensity of the higher frequency feature. For presentation, a baseline approximated by a slowly varying polynomial function was subtracted from the CW ENDOR data.

Pulsed or "echo-detected" ENDOR techniques can provide, for samples having sufficient signal/noise characteristics, advantages of increased resolution, truer line shapes, and hyperfine selectivity. In this study, a three-pulse Mims ENDOR sequence[35] [$\pi/2 - \tau - \pi/2 - t_{rf} - \pi/2 - \tau -$ echo] was used to study weakly coupled deuterons ($A(^2H) < 2$ MHz) using a locally constructed 35 GHz pulsed ENDOR instrument.[36] Typical parameters consisted of $\tau = 500$ ns, microwave $\pi/2$ $t_p = 32$ ns, rf $t_p = 60$ μs, 30 ms repetition rate, and 256 or 312 points/scan. For the Mims ENDOR sequence, hyperfine-selective "holes" in the ENDOR spectrum are expected at A-values corresponding to n/τ where $n = (1, 2, 3...)$. For $\tau =$ 500 ns, the ENDOR spectrum is thus expected to be attenuated at $A(^2H) = 2$ MHz, corresponding to $A(^1H) = 13$ MHz. In some cases pulsed ENDOR spectra were smoothed for presentation.

For a single nucleus N of $I = {}^1/_2$ coupled to the electron spin with observed hyperfine coupling A, a frozen-solution ENDOR spectrum obtained at magnetic field strength B_0 consists of a doublet at frequencies denoted ν_+ given to first order by eq 2:

$$h\nu_{\pm} = |\nu_N \pm A/2| \tag{2}$$

Depending on the relative magnitudes of A and ν_N (the nuclear Larmor frequency), the absolute value in eq 2 results in the ENDOR transitions being either centered at $A/2$ and separated by $2\nu_N$, or centered at ν_N and separated by A. Nuclei with $I > {}^1/_2$ have ENDOR spectra that are further influenced by the nuclear electric quadrupole interaction, denoted by $3P$, as described to first order by eq 3:

$$\nu_{\pm}(m_I) = |\nu_N \pm A/2 \pm (3P/2)(2m_I - 1)| \tag{3}$$

Upon isotopic substitution, A and ν_N values will be related by the ratios of g_n, as shown for $^1H/^2H$ exchange in eq 4:

(23) Hoffman, B. M.; DeRose, V. J.; Doan, P. E.; Gurbiel, R. J.; Houseman, A. L. P.; Telser, J. In *EMR of Paramagnetic Molecules*; Biological Magnetic Resonance 13; Berliner, L. J., Reuben, J., Eds.; Plenum Press: New York, 1993; pp 151−218.
(24) DeRose, V. J.; Hoffman, B. M. In *Methods in Enzymology*; Sauer, K., Ed.; Academic Press: New York, 1995; Vol. 246, pp 554−589.
(25) Telser, J.; Smith, E. T.; Adams, M. W. W.; Conover, R. C.; Johnson, M. K.; Hoffman, B. M. *J. Am. Chem. Soc.* **1995**, *117*, 5133−5140.
(26) Lowe, D. J. *Prog. Biophys. Mol. Biol.* **1992**, *57*, 1−22.
(27) Fan, C.; Gorst, C. M.; Ragsdale, S. W.; Hoffman, B. M. *Biochemistry* **1991**, *30*, 431−435.
(28) (a) Lundie, L. L.; Drake, H. L. *J. Bacteriol* **1984**, *159*, 700−703. (b) Ragsdale, S. W.; Wood, H. G. *J. Biol. Chem.* **1985**, *260*, 3970−3977. (c) Raybuck, S. A.; Bastian, N. R.; Orme-Johnson, W. H.; Walsh, C. T. *Biochemistry* **1988**, *27*, 7698- 7702. (d) Ramer, S. E.; Raybuck, S. A.; Orme-Johnson, W. H.; Walsh, C. T. *Biochemistry* **1989**, *28*, 4675- 4680.
(29) Shin, W.; Lindahl, P. A. *Biochemistry* **1992**, *31*, 12870−12875.
(30) Pelley, J. W.; Garner, C. W.; Little, G. H. *Anal. Biochem.* **1978**, *86*, 341−343.
(31) Glasoe, P. K.; Long, F. A. *J. Phys. Chem.* **1960**, *64*, 188−190.
(32) Werst, M. M.; Kennedy, M. C.; Beinert, H.; Hoffman, B. M. *Biochemistry* **1990**, *29*, 10526−10532.
(33) DeRose, V. J.; Liu, K. E.; Lippard, S. J.; Hoffman, B. M. *J. Am. Chem. Soc.* **1996**, *118*, 121- 134.
(34) Hoffman, B. M.; DeRose, V. J.; Ong, J.-L.; Davoust, C. E. *J. Magn. Reson. Ser. A* **1994**, *110*, 52−57.
(35) Mims, W. B. *Proc. R. Soc. London* **1965**, *283*, 452−457.
(36) Davoust, C. E.; Doan, P. E.; Hoffman, B. M. *J. Magn. Reson.* **1996**, *119*, 38−44.

$$\boldsymbol{A}(^1\mathrm{H})/\boldsymbol{A}(^2\mathrm{H}) = \boldsymbol{g}_n(^1\mathrm{H})/\boldsymbol{g}_n(^2\mathrm{H}) = 6.51 \quad (4)$$

The observed hyperfine coupling A includes both isotropic and anisotropic terms, where A_{iso} is the average of the three principal hyperfine tensor components (A_1, A_2, A_3). We have developed procedures for determining complete hyperfine and quadrupole tensors by collecting ENDOR spectra across the EPR envelope and analyzing them, as described.[23] For the CODH C-cluster, however, low EPR signal intensities, broad line widths, and interference from B-cluster EPR signals made full ENDOR analyses problematic and an approximate field-dependent analysis was possible only in the case of the ^{57}Fe ENDOR. In addition, the lowest C-cluster $\boldsymbol{g}$-values ($g < \sim 1.7$, $H > \sim 14\,700$ G) could not be observed because of magnetic field strength limitations of the 35 GHz CW ENDOR spectrometer. When available, general field-dependent trends for the observed hyperfine couplings are described.

Results and Analysis

35 GHz EPR Spectra of the CODH$_{Ct}$ C-Cluster. Figure 1 displays the EPR absorption envelope, obtained at 35 GHz, of CODH$_{Ct}$ samples poised in the C_{red1} ($\boldsymbol{g} = [2.01, 1.81, 1.65]$), $C_{red1}(CN^-)$ ($\boldsymbol{g} = [1.87, 1.78, 1.55]$), and C_{red2} ($\boldsymbol{g} = [1.97, 1.87, 1.75]$) states. C_{red1} can be formed in the absence of other EPR-active states of CODH$_{Ct}$, yielding a clean spectrum as shown in Figure 1a. The signal observed with CN^- treatment shown in Figure 1b has small contributions from B_{red} ($\boldsymbol{g} = [2.04, 1.94, 1.90]$) and reduced center A ($g > 2$). Significant amounts of B_{red} are present in samples poised to yield the C_{red2} state of the C-cluster (Figure 1c). Fortunately, EPR signals from the different clusters of CODH$_{Ct}$ do not overlap completely,[37] and ENDOR spectra obtained at higher magnetic field values corresponding to $g \leq 1.87$ probe only the C-cluster. To compare between states of the C-cluster, ENDOR spectra were obtained at g_2 for all species, and also at higher fields corresponding to $g \leq 1.75$.

^{1}H and ^{2}H ENDOR of C_{red1} and C_{red2}. At $g = 1.72$, the CW C_{red1} proton ENDOR pattern includes a broad resonance with $A_{max}(^1H_s) = 16$ MHz, denoted H_s, that is lost upon exchange into D_2O (Figure 2a). This proton is not present in samples poised as C_{red2} (Figure 2b) or inhibited with CN^- (Figure 2c). The hyperfine coupling to H_s is highly anisotropic, and the features due to H_s show a maximum splitting and are sharpest at $g \leq 1.7$; the proton ENDOR pattern at the low-field edge (g_1) of the C_{red1} EPR spectrum extends only to $A_{max}(^1H) \approx 8$ MHz (data not shown).

The C_{red1} proton ENDOR spectra also exhibit a class of moderately coupled, exchangeable protons denoted H_m. Due to spectral overlap with nonexchangeable resonances, these protons are not readily apparent through comparison of the ^{1}H ENDOR spectra of C_{red1} or C_{red2} in H_2O and D_2O. However, they are clearly observed by pulsed or "echo-detected" Q-band ^{2}H Mims ENDOR. Samples prepared in D_2O reveal a ^{2}H pattern centered at the Larmor frequency of $\nu_N(^2H) \approx 8$ MHz for C_{red1}, C_{red2}, and CN^--inhibited samples (Figure 3) whose widths of $\sim$1.2 MHz at g_2 correspond to maximum proton couplings of $A(^1H_m) = 7-8$ MHz.[38] At higher field values corresponding to $g < 1.7$, the ^{2}H ENDOR spectrum of C_{red1} (Figure 3a) sharpens and H_m resolves into peaks at $\nu_N(^2H) \pm 0.2$ and ± 0.45 MHz, corresponding to exchangeable protons with $A(^1H) = 2.6$ and 6 MHz, respectively. The latter in fact can be observed in the proton ENDOR spectra of C_{red1} (vertical arrow at $A(^1H)/2 = +3$ MHz in Figure 2a).

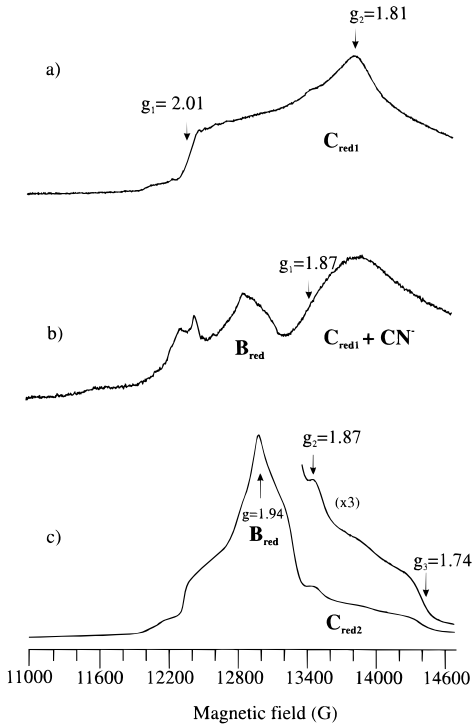

Figure 1. 35 GHz EPR spectra of CODH$_{Ct}$. EPR spectra are shown for CODH poised in the (a) C_{red1} (pH 8.0), (b) C_{red1} (CN^-), and (c) C_{red2} states. In each case the rapid-passage dispersion-detected spectrum is shown, giving an absorptive lineshape. Spectrometer conditions: 2 K, 1.3 G (100 kHz) magnetic field modulation.

In addition to the exchangeable protons H_s and H_m, several pairs of resonances from nonexchangeable protons also are observed in the ^{1}H ENDOR spectra of the C-cluster (Table 2). Proton ENDOR spectra taken at different magnetic fields across the EPR spectrum reveal a pattern that includes at least five partially resolved pairs with maximum couplings of $A(^1H) = 11$ MHz at g_2 (data not shown). The ^{1}H ENDOR patterns for both C_{red2} and $C_{red1}(CN^-)$ show similar properties, although the ^{1}H couplings and resolutions differ between samples poised in the different states. These strongly coupled, nonexchangeable protons likely are attached to β-carbons of cysteinyl thiolates coordinated to the C-cluster.[39]

Assignment of Exchangeable Protons. Exchangeable protons associated with an $[Fe_4S_4]$ center such as that in the

(37) In many reported X-band EPR spectra, temperature and power variations have been used to separate the CODH EPR signals on the basis of their different relaxation properties. Under the low-temperature rapid-passage conditions used in this study, all of the species present contribute to the absorption-like EPR envelope. ENDOR spectra at any field value would be the sum of features due to each contributing species in the EPR spectrum.

(38) (a) Mims pulsed ENDOR spectra are sensitive to microwave pulse interval τ and have undistorted line shapes under conditions of $A < 1/(2\tau)$, which for the CODH ^{2}H ENDOR data presented here corresponds to $A(^2H) < \sim 1$ MHz (see Methods and the discussions in Willems et al. (ref 38b) and Doan et al. (ref 39a)). Therefore, the conditions of the ^{2}H Mims pulsed ENDOR data displayed in Figure 3 are sensitive only for the weakly coupled deuterons corresponding to H_m, and the $A(^2H) = 2.5$ MHz deuterons corresponding to substituted H_s are, as expected, not observed. Limited data obtained using the ReMims sequence (ref 38c), which gives further control over line shape distortions, confirmed the hyperfine results for H_m (data not shown). (b) Willems, J.-P.; Lee, H.-I.; Burdi, D.; Doan, P. E.; Stubbe, J.; Hoffman, B. M. *J. Am. Chem. Soc.* **1997**, *119*, 9816−9824. (c) Doan, P. E.; Hoffman, B. M. *Chem. Phys. Lett.* **1997**, *269*, 208−214.

(39) (a) Doan, P. E.; Fan, C.; Hoffman, B. M. *J. Am. Chem. Soc.* **1994**, *116*, 1033−1041. (b) Mouesca, J.-M.; Rius, G.; Lamotte, B. *J. Am. Chem. Soc.* **1993**, *115*, 4714−4731.

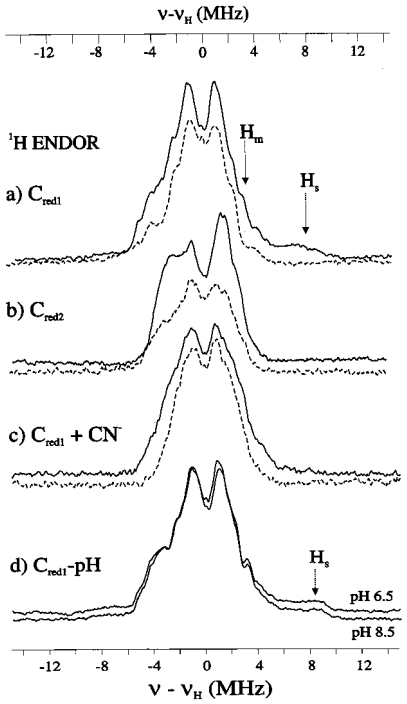

Figure 2. Proton ENDOR spectra obtained at g_3 for $CODH_{Ct}$ poised in the C_{red1} and C_{red2} states. CW 35 GHz proton ENDOR spectra, obtained at g-values near to g_3, are shown for samples of $CODH_{Ct}$ poised as (a) C_{red1}, (b) C_{red2}, and (c) $C_{red1}(CN^-)$. Spectra are shown centered at the proton Larmor frequency (ν_H) for each magnetic field value. Unless specified, samples were poised at pH = 7.5. Dotted lines indicate samples prepared in ^2H_2O buffer. The vertical arrows indicate couplings assigned to two classes of exchangeable protons denoted H_m and H_s, the latter of which is absent in samples poised as C_{red2} or following addition of CN^- to C_{red1}. The spectra in d are of C_{red1} samples poised at pH 6.5 and 8.5 and indicate that the appearance of H_s is independent over this range of pH. Spectrometer conditions: CW proton ENDOR spectra were obtained with an rf sweep rate of 2 MHz/s (negative sweep) and a magnetic field modulation amplitude of 0.6 G: (a) 14 600 G, 35.060 GHz (H_2O), 35.121 GHz (D_2O); (b) 14 600 G, 35.075 GHz; (c) 14 600 G, 35.080 GHz; (d) (pH 6.5) 14 608 G, 35.011 GHz; (pH 8.5) 14 600 G, 35.065 GHz. Each spectrum is the average of 100−140 scans.

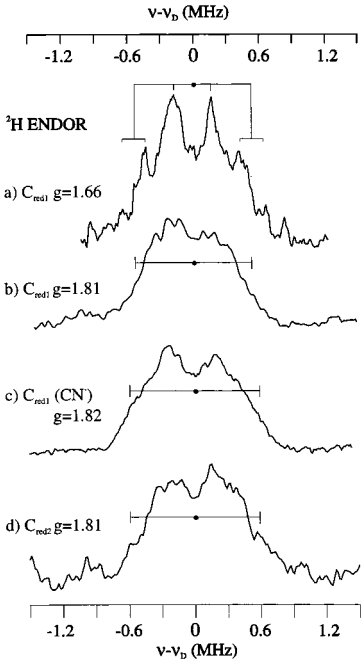

Figure 3. Deuteron ENDOR spectra of $CODH_{Ct}$ poised in the C_{red1} and C_{red2} states. Pulsed 35 GHz deuteron ENDOR spectra are shown for $CODH_{Ct}$ prepared in ^2H_2O buffer and poised in the (a, b) C_{red1}, (c) C_{red1} (CN^-), and (d) C_{red2} forms. Pulsed ENDOR spectra were obtained using a Mims pulsed ENDOR sequence (see Methods) under the following conditions: (a) 15 000 G, 34.806 GHz, 10 scans; (b) 13 720 G, 34.757 GHz, 28 scans; (c) 13 630 G, 34.729 GHz, 9 scans; (d) 13 690 G, 34.689 GHz, 28 scans.

Table 2. Observed Hyperfine Couplings[a] at $g = 1.75$ for $CODH_{Ct}$ Poised in the C_{red1} and C_{red2} States

		C_{red1}	C_{red2}
^1H	nonexchangeable	1.6, 2.4, 4.2, 8.0,	1.8, 2.4, 3.0,
	exchangeable	2.6,[b] 6.0,[b] 16	4.6, 6.0, 8.0[b]
^{14}N		7.8 (1.2)[c]	8.4 (2.4)[c]

[a] Couplings reported in MHz. Errors due to line width and sweep artifacts are approximately ±0.3 MHz. [b] Maximum hyperfine couplings of exchangeable protons derived from overall width of ^2H resonances. [c] Numbers in parentheses are ^{14}N quadrupole splitting parameters 3P (MHz) as observed at $g = 1.75$.

C-cluster could be attached to a terminal ligand of an Fe ion, or be involved in hydrogen bonding to the cluster sulfur atoms such as through amide-N−H···S interactions. Hydrogen-bonded protons in the $[Fe_3S_4]^{1+}$ cluster from *D. gigas* hydrogenase have been studied by ENDOR and have a range of observed hyperfine couplings extending to $A(^1H) = 9$ MHz.[39a,40] At physiological pH values, hydroxide or water (H_xO) species are the most likely terminal ligands containing an exchangeable proton in the first coordination sphere. Previously reported proton hyperfine couplings for terminal aqueous ligands to high-spin Fe include $A(^1H) = 8$ MHz for the ferrous site of the methane monooxygenase dinuclear Fe center[33] and $A(^1H) = 10-15$ MHz for the ferric hemes in chloroperoxidase and cytochrome P_{450}.[41] The $A(^1H) = 6-8$ MHz coupled protons (H_m) observed by ^2H ENDOR in C_{red1}, C_{red2}, and $C_{red1}(CN^-)$ remain essentially unchanged in all three C-cluster states, and so we provisionally assign H_m to hydrogen bonds about the $[Fe_4S_4]^{1+}$ center. The magnitude of $A(^1H) \approx 16$ MHz for the strongly coupled proton (H_s), however, is larger than any proton coupling reported for a hydrogen bond in an Fe−S cluster, and a more reasonable assignment for H_s is to a proton of a terminal ligand.

To make structural predictions based on observed hyperfine couplings in a multinuclear spin center, such as in the $[Fe_4S_4]^{1+}$ center, the electron spin coupling must be taken into account. This is accomplished by using the relation $(A_{obs})_i = a_{int}K_i$, where (A_{obs}) is the observed hyperfine coupling at Fe_i, a_{int} is the intrinsic (site) coupling, and K_i is a coefficient that gives the spin projection at Fe_i. A value of $K_{FCII} = -1.3$ can be derived for FCII by applying the spin-coupling model described by Mouesca et al.[42] to the published Mössbauer parameters for the $CODH_{Rr}$ C-cluster (in the C_{red1} state).[5,43] Assuming purely dipolar coupling and a simple point-dipole approximation for

(40) Fan, C.; Teixeira, M.; Moura, J.; Moura, I.; Huynh, B.-H.; Le Gall, J.; Peck, H. D., Jr.; Hoffman, B. M. *J. Am. Chem. Soc.* **1991**, *113*, 20−24.

(41) Fann, Y.-C.; Gerber, N. C.; Osmulski, P. A.; Hager, L. P.; Sligar, S. G.; Hoffman, B. M. *J. Am. Chem. Soc.* **1994**, *116*, 5989−5990.

(42) Mouesca, J.-M.; Noodleman, L.; Case, D. A.; Lamotte, B. *Inorg. Chem.* **1995**, *34*, 4347−4359.

(43) The spin projection coefficients K_i for each Fe atom of C_{red1} can be derived from $K_i = A^{exp}/a_{iso}$ using the analysis procedure of Mouesca et al. (ref 42). Values for A^{exp} are taken from the C_{red1} isotropic ^{57}Fe hyperfine couplings obtained by Mössbauer studies of CODH from *R. rubrum* (ref 5, listed in Table 3). We assume intrinsic $a_{iso}(^{57}Fe)$ values of −22.5 and −18 MHz for $Fe^{2.5+}$ and Fe^{2+}, respectively (ref 42). For the mixed-valent pair of C_{red1}, $A^{exp}(Fe^{2.5}) = -37.2$ MHz and $K_{mv} = A^{exp}(Fe^{2.5})/a_{iso}(Fe^{2.5}) = +1.65$. Similarly, $K_{FCII} = -1.33$ for FCII and $K_{FCIII} = -0.98$ for FCIII. As expected, $\sum_i K_i = 0.99 \approx 1$.

coupling between H_s and FCII, a maximum of $A_{obs}(^1H) = 16$ MHz then gives an effective distance of $r \approx 2.3$ Å for H_s. This short distance is most consistent with a hydroxide or water ligand on FCII.[44,45] The loss of the signal upon CN^- binding suggests that cyanide, proposed to bind to FCII, replaces the bound H_xO ligand.

Effect of pH on C_{red1} and C_{red2} ^{1}H ENDOR. A previous study had suggested that the C_{red1} state of the C-cluster bound a catalytically relevant protonated ligand, such as H_2O, with a pK_a of ~7.2,[21] and we considered whether the strongly coupled H_s proton was associated with this species. Proton ENDOR data were obtained for C_{red1} samples prepared at pH 6.5 and 8.5 as well as at pH 7.5 (Figure 2a). The proton hyperfine pattern of C_{red1}, including the features due to H_s, is essentially unchanged over this pH range (Figure 2d). Proton ENDOR scans performed under conditions of higher resolution furthermore show that protons with couplings $A(^1H) < 6$ MHz also are not affected by these pH changes (data not shown). Corresponding spectra of C_{red2} also were similarly invariant with pH (data not shown).

^{14}N ENDOR of C_{red1} and C_{red2}. The low-frequency region of the ENDOR spectrum of C_{red1}, observed at $g = 1.75$, exhibits relatively sharp resonances at 7.6 and 8.9 MHz (Figure 4b) that are in the frequency range expected for ^{14}N signals. Equivalent spectra of C_{red2} exhibit resonances at 7.4 and 9.7 MHz (Figure 4a). As indicated in Figure 4 these resonances of both C_{red1} and C_{red2} can each be assigned to a strongly coupled ^{14}N, with $A(^{14}N) \approx 8$ MHz.[46] ^{14}N ENDOR features previously have been observed for Fe−S centers under two circumstances: from directly coordinated histidyl ligands (in the case of the Rieske proteins[47,48]) and from ^{14}N of peptide amides that are hydrogen bonded to cluster sulfides.[49,50] The hyperfine couplings in the second case are $A(^{14}N) < 3$ MHz, much smaller than those observed here.[51] Histidine is the only nitrogenous ligand identified so far for Fe−S centers, and His ligands have been definitively identified in the Rieske [Fe_2S_2] center[47,48] and the distal [Fe_4S_4] center of *D. gigas* Ni−Fe hydrogenase.[52] Hyperfine values of $A_{iso}(^{14}N) = 4-6$ MHz were determined from ENDOR studies of the Rieske center;[47,48] the *D. gigas* distal [Fe_4S_4] center has not been studied by ENDOR. Observed values for histidine ligands to the ferrous site in dinuclear Fe^{oxo} spin-coupled clusters also are $A(^{14}N)$ 4−6 MHz.[33] Hence, the ^{14}N resonances observed for both C_{red1} and C_{red2} are consistent with a histidine ligand to the C-cluster.

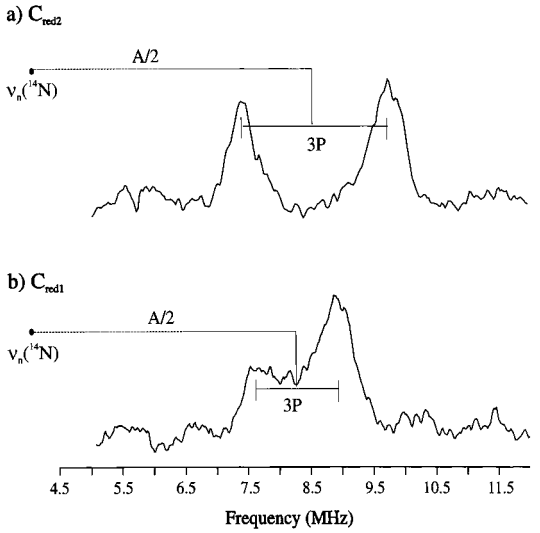

Figure 4. ^{14}N ENDOR of C_{red1} and C_{red2}. CW ENDOR, obtained near g_3, of natural-abundance $CODH_{Ct}$ samples poised in the (a) C_{red2} and (b) C_{red1} forms. ^{14}N ENDOR assignments are indicated as centered at $\nu_n(^{14}N)$ (closed circles) and separated by $A/2$ and $3P$. Spectrometer conditions: CW ENDOR spectra were obtained with an rf sweep rate of 1 MHz/s (negative sweep) and a magnetic field modulation amplitude of 1.3 G: (a) 14 350 G, 35.152 GHz, 130 scans; (b) 14 320 G, 35.074 GHz, 170 scans.

^{57}Fe ENDOR of C_{red1} and C_{red2}. ^{57}Fe-enriched samples of $CODH_{Ct}$ were examined by ENDOR to investigate the electronic differences between C_{red1} and C_{red2}. ^{57}Fe ENDOR spectra of samples poised in each state were acquired at several field positions across the EPR envelope. The field-dependent data and assignments are given in the Supporting Information, and representative spectra acquired at g_2 are shown in Figure 5. In Figure 5a, the partially resolved features of the C_{red1} ^{57}Fe spectrum are assigned to the ν_+ branches (with ν_+ dominant) of two classes of iron having $A(^{57}Fe_1) = 31$ MHz and $A(^{57}Fe_2) = 37$ MHz at this g-value. For C_{red2}, the data generally showed less resolution, but two approximate $A(^{57}Fe)$ values also can be assigned, as shown in Figure 5b. The two approximate

(44) Assuming *only* dipolar coupling and the point-dipole approximation, an observed $A(^1H) = 16$ MHz for an exchangeable proton near to FCII ($K_{FCII} = -1.3$) would correspond to $A_{dip}(^1H) = |16/(-1.3)| = 12.3$ MHz. A proton at distance r from the electron spin has a through-space dipolar coupling of magnitude $A_{dip} = g_N\beta_n g_e\beta_e(3\cos^2\theta - 1)(1/r^3) = (79)(2)(1/r^3)$ at its maximum value. This gives a lower limit of $r \geq 2.3$ Å for the distance between FCII and the strongly coupled proton, which is very reasonable for the proton of a H_xO ligand to that iron. The assumption of negligible isotropic coupling is reasonable on the basis of previous successful analyses of other high-spin Fe(III)−aqua/hydroxo complexes by ENDOR (refs 38b, 44a). Invoking a small $A_{iso}(^1H) \approx 2$ MHz (ref 44b) and $A_{obs} = A_{iso} + A_{dip}$ increases the estimated distance to $r > 2.45$ Å, which is still well within a reasonable metal−proton distance for a terminal aqueous ligand. We note that it is possible to draw a structure in which an approximate minimal distance of $r \approx 2.4$ Å could be attained between FCII and the proton of a Ni-bound OH^- ligand, assuming a single atom bridge between the two metals and a metal−metal distance of ~3 Å. However, this model would require a particularly fortuitous alignment of atoms and is considered a less likely source of H_s. (a) Mulks, C. F.; Scholes, C. P.; Dickinson, L. C.; Lapidot, A. *J. Am. Chem. Soc.* **1979**, *101*, 1645−1653. (b) LoBrutto, R.; Scholes, C. P.; Wagner, G. C.; Gunsalus, I. C.; Debrunner, P. G. *J. Am. Chem. Soc.* **1980**, *102*, 1167−1170.

(45) Although this analysis is very approximate, the assignment is strongly supported by recent ^{1}H and ^{2}H ENDOR studies of the exchangeable protons of substrate-free aconitase. These new ENDOR measurements (H. I. Lee, B. M. Hoffman, M. C. Kennedy, unpublished results) show that for the hydroxyl ligand of Fe_a, the maximum hyperfine couplings also extend to $A(^1H) = 16$ MHz, which is larger than the previously reported value of 8 MHz (ref 32).

(46) (a) The ^{14}N peaks can be assigned as quadrupole-split resonances from the ν_+ doublet, with [$A(^{14}N) = 8.3$ MHz, $3P = 2.3$ MHz] for C_{red2} and [$A(^{14}N) = 7.7$ MHz, $3P = 1.3$ MHz] for C_{red1} as observed at $g = 1.75$. The ν_- partners of these doublets would appear at <3 MHz and were not detected. These observed values of $3P$ are well within the range expected for histidine imino nitrogen coordination (ref 46b) and measured for other high-spin Fe(III)−histidine interactions (for example, refs 33, 47, 48). The different *observed* quadrupole splittings in C_{red1} and C_{red2} are likely due to different orientations of $\boldsymbol{g}$, $\boldsymbol{A}$, and $\boldsymbol{P}$ at the observing magnetic field position rather than large chemical differences between ^{14}N in the two states. (b) Ashby, C. I. H.; Cheng, C. P.; Brown, T. L. *J. Am. Chem. Soc.* **1978**, *100*, 6057−6067.

(47) Gurbiel, R. J.; Batie, C. J.; Sivaraja, M.; True, A. E.; Fee, J. A.; Hoffman, B. M.; Ballou, D. P. *Biochemistry* **1989**, *28*, 4861−4871.

(48) Gurbiel, R. J.; Doan, P. E.; Gassner, G. T.; Macke, T. J.; Case, D. A.; Ohnishi, T.; Fee, J. A.; Ballou, D. P.; Hoffman, B. M. *Biochemistry* **1996**, *35*, 7834−7845.

(49) Houseman, A. L. P.; Oh, B.-H.; Kennedy, M. C.; Fan, C.; Werst, M. M.; Beinert, H.; Markley, J. L.; Hoffman, B. M. *Biochemistry* **1992**, *31*, 2073−2080.

(50) Adman, E.; Watenpaugh, K. D.; Jensen, L. H. *Proc. Natl. Acad. Sci. U.S.A.* **1975**, *72*, 4854−4848.

(51) The data of Figure 4 do not give reasonable fits to the familiar expression for ^{14}N $\Delta m = \pm 2$ "double quantum" transitions previously observed by Q-band ENDOR for other Fe−S centers that lack direct nitrogen ligands (ref 49).

(52) Volbeda, A.; Charon, M.-H.; Piras, C.; Hatchikian, E. C.; Frey, M.; Fontecilla-Camps, J. C. *Nature* **1995**, *373*, 580−587.

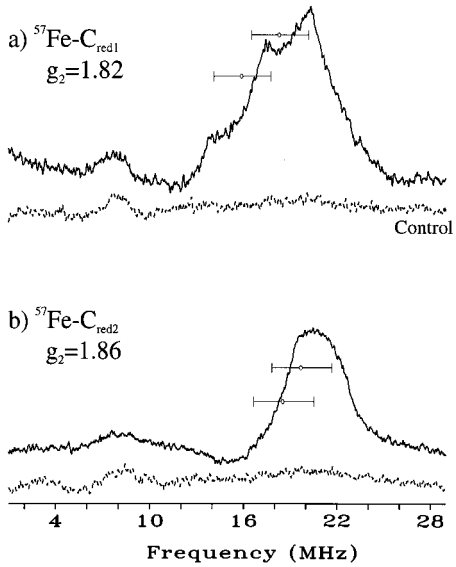

Figure 5. ^{57}Fe ENDOR of $CODH_{Ct}$. CW ENDOR of samples enriched in ^{57}Fe and poised in the (a) C_{red1} and (b) C_{red2} forms, obtained at g_2. The dotted lines show the backgrounds from natural-abundance samples of C_{red1} and C_{red2}, respectively. ^{57}Fe ENDOR assignments are indicated centered at $A(^{57}Fe)/2$ (open circles) and separately by $2\nu_n(^{57}Fe)$ (= 3.8 MHz at these magnetic fields, horizontal bars). Spectrometer conditions: CW ENDOR spectra were obtained with an rf sweep rate of 1 MHz/s (negative sweep) and a magnetic field modulation amplitude of 0.5 G. Each spectrum is the average of 100 scans: (a) 13 530 G; (b) 13 800 G (both spectra).

Table 3. ^{57}Fe Hyperfine Couplings Observed for $CODH_{Ct}$ Poised in the C_{red1} and C_{red2} States[a]

state[a]	Fe site	$A(^{57}Fe)$, A_{iso} (MHz)
C_{red1}	FCIII(Fe^{2+}) Mössbauer[b]	[7, 15, 31,], 18
	FCII(Fe^{2+}) Mössbauer[b]	[13, 18, 41], 24
	$(Fe^{2.5+})_2$ Mössbauer[b]	[−31, −41, −40], −37
	ENDOR[c,d]	[32, 37, 44], 38
		[24, 31, 41], 32
C_{red2}	$(Fe^{2.5+})_2$ ENDOR[c,e]	[−, ∼36, 46]
		[−, ∼36, 41]

[a] Mössbauer parameters are for $CODH_{Rr}$ (ref 5); ENDOR for $CODH_{Ct}$ (this work). [b] Mössbauer-determined $\boldsymbol{A}(^{57}Fe)$ tensors have no spatial relationship to the $\boldsymbol{g}$ tensor. The hyperfine tensor components are given in the order A_x, A_z, A_y for FCII and FCIII and in the order A_x, A_y, A_z for $(Fe^{2.5+})_2$. This provides better correspondence to the tensors determined by ENDOR, which are given in the order A_{g_1}, A_{g_2}, A_{g_3}, where for C_{red1}, $\boldsymbol{g} = [g_1, g_2, g_3] = [2.01, 1.81, 1.65]$. [c] The ENDOR-determined $\boldsymbol{A}(^{57}Fe)$ tensors are assumed collinear with the $\boldsymbol{g}$ tensor. No sign information is obtainable from ENDOR and values are accurate to ±0.5 MHz. The assignment to Fe site is tentative (see the Supporting Information). [d] ENDOR spectra for C_{red1} were recorded near but not at g_3 due to magnetic field limitations. [e] No values were determined for C_{red2} at g_1 due to spectral overlap with ^{57}Fe signals from B_{red}.

$A(^{57}Fe)$ tensor components derived by field-dependent ENDOR (Supporting Information) for each $CODH_{Ct}$ C-cluster state are listed in Table 3. Comparison of the estimated hyperfine tensors for the two Fe ions of C_{red1} and C_{red2} with values determined by Mössbauer for $CODH_{Rr}$ poised in the C_{red1} state[5] indicates that the ions observed here by ENDOR are the two members of the mixed-valent pairs $[(Fe^{2.5+})_2]$. As conveniently summarized by Mouesca et al.,[42] the two types of Fe generally found for standard $[Fe_4S_4]^{1+}$ clusters in protein and model compounds are characterized by observed isotropic hyperfine couplings of $A_{iso}(Fe^{2.5+}) \approx -30$ MHz for the mixed-valence pair and $A_{iso}(Fe^{2+}) \approx +15$ MHz for the ferrous ions. As is the case with aconitase, the value of $|A_{iso}(Fe^{2.5+})| \approx 38$ MHz in the C-cluster is significantly higher than the value of 30 MHz seen in typical $[Fe_4S_4]^{1+}$ clusters. Overall, the ^{57}Fe ENDOR data show that C_{red1} and C_{red2} are broadly similar to each other, yet significantly different from typical $[Fe_4S_4]^{1+}$ clusters.

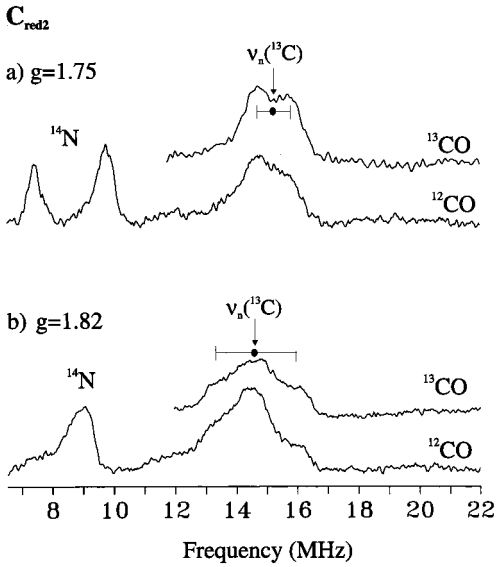

Figure 6. ^{13}C ENDOR of $CODH_{Ct}$ poised in the C_{red2} state using ^{13}CO or ^{12}CO. Samples were poised in the C_{red2} form by reduction with either ^{13}CO (upper traces) or natural abundance (lower traces) CO (see Methods). ^{13}C ENDOR assignments for the natural abundance ^{13}C present in both samples are centered at $\nu_n(^{13}C)$ (solid circles) and separated by $A(^{13}C)$ (horizontal bars). No additional ^{13}C signals are detected for samples poised using ^{13}CO. Data were obtained near (a) $g_3 = 1.75$ or (b) $g_2 = 1.82$. Spectrometer conditions: CW ENDOR spectra were obtained with an rf sweep rate of 1 MHz/s (negative sweep) and a magnetic field modulation amplitude of 1.3 G: (a) 14 390 G, 233 scans (^{13}CO); 14 350 G, 245 scans (^{12}CO); (b) 13 840 G, 100 scans (^{13}CO); 13 800 G, 130 scans (^{12}CO).

^{61}Ni ENDOR. We examined several concentrated ^{61}Ni -enriched samples of C_{red1} and C_{red2}, under CW and pulsed conditions, and at multiple magnetic fields. No signals attributed to ^{61}Ni ENDOR were observed in either state of our ^{61}Ni-enriched samples. In contrast, ^{61}Ni ENDOR was readily observed for CO-reduced center A of $CODH_{Ct}$.[27] The absence of such resonances for the C-cluster supports the conclusion of Hu et al.[5] that the Ni is at most weakly coupled to the electronic spin of C_{red1} or C_{red2}.

^{13}C ENDOR of C_{red1} and C_{red2}. The C_{red1}-to-C_{red2} conversion is not completely understood, and one possibility, proposed by Kumar et al.,[9] is that the C_{red2} state results when CO binds to C_{red1}. To test for this possibility, we reduced $CODH_{Ct}$ with ^{13}CO and searched for corresponding ^{13}C ENDOR features. Both ^{12}CO- and ^{13}CO-reduced samples show identical signals that are centered at the ^{13}C Larmor frequency ($\nu_N(^{13}C) = 13-15$ MHz at these magnetic field values) and that correspond to couplings of $A(^{13}C) = 1-2$ MHz (Figure 6). These likely are from natural-abundance ^{13}C of the β-carbons of cysteinyl residues, as shown earlier in ENDOR studies of Fe−S clusters.[49] As illustrated in Figure 6, the ENDOR spectra of the C_{red2} state prepared with ^{13}CO also show no additional features. In contrast, ^{13}C ENDOR signals with strong, mainly isotropic, hyperfine couplings ($A(^{13}C) = 30$ MHz) were readily detected from ^{13}CO bound to the $CODH_{Ct}$ A-cluster.[27] Other Fe−S systems in which ^{13}C ENDOR due to bound ^{13}CO was readily observed include oxidized *Clostridium pasteurianum* hydrogenases I and II ($A(^{13}C) = 20-34$ MHz);[53,54] and intermediates

(53) Telser, J.; Benecky, M. J.; Adams, M. W. W.; Mortenson, L. E.; Hoffman, B. M. *J. Biol. Chem.* **1986**, *261*, 13536−13541.

of the MoFe protein of nitrogenase, trapped during CO-inhibition ($A(^{13}C) < \sim 6$ MHz).[55] Moreover, the isoelectronic cyanide ion shows strong ^{13}C coupling in ^{13}CN-treated C_{red1} samples ($A(^{13}C) \approx 13$ MHz at $g = 1.81$).[8] The absence of detectable ^{13}C ENDOR signals from the ^{13}CO-treated C_{red2} thus strongly suggests that CO is not bound to the $[Fe_4S_4]^{1+}$ component of C_{red2}. Because the Ni component of the C-cluster is not strongly coupled to the electron spin of the C-cluster, these results do not exclude the possibility that CO is bound to the Ni center in the C_{red2} state.

Discussion

Evidence for an H_xO Ligand on the $[Fe_4S_4]$ Component of the C-cluster. In its one-electron reduced form, C_{red1}, the CODH C-cluster exhibits ENDOR resonances due to a strongly coupled, exchangeable proton denoted here as H_s. The maximum coupling of $A(^1H) = 16$ MHz observed for H_s is consistent with its assignment to a H_xO ($x = 1,2$) ligand bound to an Fe atom of the $[Fe_4S_4]^{1+}$ cluster. Because the ^1H ENDOR signal is lost upon treatment with CN^-, which likely binds to FCII,[5] we provisionally assign H_s as due to H_xO coordinated specifically to FCII.

When the C-cluster is further reduced to C_{red2}, the species giving rise to H_s also appears to be lost. The CO oxidation model proposed by Hu et al.[5] is based on a heterobimetallic catalytic site in which the FCII−X−Ni unit binds the OH^- and CO substrates to Fe and Ni, respectively. It is thought that C_{red2} represents the state of the C-cluster following CO-oxidation, and so the presence of an H_xO ligand to FCII in C_{red1} and its absence in C_{red2} support the involvement of an OH^--bound FCII in catalysis. Reduction of the cluster to C_{red2} with ^{13}CO generates no new ENDOR resonances from ^{13}C, strongly suggesting that neither CO nor its oxidation products remain bound to the $[Fe_4S_4]$ cluster in the C_{red2} state. The lack of detectable ^{61}Ni ENDOR in the C-cluster indicates that the unpaired electron spin is localized on the $[Fe_4S_4]$ cluster, and thus either the Ni^{2+} is $S = 0$ or the bridge mediates negligible exchange coupling. Under these circumstances, we cannot determine by ENDOR whether CO might be bound to the Ni ion in C_{red2}.

CN^- treatment of the $CODH_{Ct}$ C-cluster results in an EPR signal that is significantly altered and broadened, with a decrease from $g_{av} = 1.82$ for C_{red1} to $g_{av} = 1.72$ in $C_{red1}(CN^-)$. ^{13}C ENDOR from $^{13}CN^-$-treated CODH[8] and Mössbauer studies[5] both lead to the conclusion that CN^- binds to FCII of the C-cluster in the C_{red1} state. Since the H_s ENDOR signal is absent in spectra of CN^--inhibited CODH, it is reasonable to propose that CN^- inhibits CO oxidation activity in CODH by displacing catalytically essential OH^- that is bound to FCII. The magnitude of the effect of CN^- on the spectroscopic properties of the C_{red1} state further suggests that cyanide causes additional changes in ligand geometry at FCII beyond replacing the terminally bound H_xO ligand in C_{red1}.

Formation of C_{red2} causes lesser electronic changes in the C-cluster $[Fe_4S_4]$ center than does CN^- treatment. The similarity in g-values and in highest observed values of $A(^{57}Fe)$ (Table 3) for C_{red1} and C_{red2}, plus preliminary indication that the Mössbauer parameters of FCII remain relatively unchanged,[5] all suggest relatively minor geometric differences between C_{red1} and C_{red2}. However, C_{red2} has lost the H_xO ligand of C_{red1} and additionally is thought not to bind CN^-.[6] Thus it appears that reduction of the C-cluster from C_{red1} to the C_{red2} state creates only minor structural perturbations at the $[Fe_4S_4]$ cluster, but results in a configuration in which the unique Fe ion apparently is protected from binding by small diatomic anions.

The C-cluster Has a Nitrogenous Ligand. Resonances from a relatively strongly coupled ^{14}N are found in the ENDOR spectra of both C_{red1} and C_{red2}. The strength of the hyperfine coupling ($A(^{14}N)_{obs} \approx 8$ MHz at $g = 1.75$) indicates that it arises from a ligated molecule. Although we cannot rule out other sources at this time, histidine is by far the most common nitrogenous metalloprotein ligand and is the only N-donor ligand observed so far for Fe−S centers. Substitution of a neutral histidine ligand for an anionic cysteine ligand appears to result in an increased redox potential of Fe−S centers, as is seen for the Rieske-type $[Fe_2S_2]^{2+/1+}$ clusters coordinated with two histidine ligands ($E^{0'} = -100$ to $+400$ mV)[47,48,56] and the distal $[Fe_4S_4]^{2+/1+}$ cluster in *D. gigas* hydrogenase (reported $E^{0'}$ values of -255 mV[57] and -270 mV[58] (pH 7.0)), shown by X-ray crystallography to have one histidine ligand.[52] For the C-cluster, histidine coordination may thus contribute to the fact that the reduction potential for the C_{ox}/C_{red1} couple (reported values of $E^{0'} = -220$ mV for $CODH_{Ct}$ and -110 mV for $CODH_{Rr}$) is 200−300 mV higher than those of standard $[Fe_4S_4]^{2+/1+}$ clusters.

A Model for the C-cluster

Figure 7a represents the most probable current model of the C-cluster's coordination environment in the C_{red1} state. The unique iron, FCII, is shown coordinated by the three sulfide ions of the cluster, a histidine, a terminal hydroxyl group, and an unidentified bridging ligand.[59] The remaining three irons are assumed to be coordinated to cysteines, consistent with the ^1H ENDOR data. The model illustrates the probable hydrogen bonding (resulting in the H_m protons detected by ENDOR) between the sulfurs of the cluster and the peptide backbone. The Ni is assumed to be trigonal bipyramidal, with the sixth site reserved for binding the substrates CO and CO_2. This geometry is suggested both by Ni XAS of $CODH_{Rr}$,[18] and by theoretical studies of Ni^{2+}−CO binding.[60] Ni EXAFS indicates 2−3 N/O donors and 2 S donors.[18] Two of these N/O donors to Ni are presumed to be histidine and the bridge to the cluster. A hypothetical redox-active ligand L (see Introduction) also is included.

This C-cluster model is supported by the amino acid sequence homology among several Ni-containing CODH's: monomeric $CODH_{Rr}$, the β subunit of $CODH_{Ct}$, and the α subunit of $CODH_{Ms}$. Kerby et al.[3] have compared the amino acid sequences of these three polypeptides and find that the sequence of $CODH_{Rr}$ is 67% similar to the β subunit of $CODH_{Ct}$ and 47% similar to the α subunit of $CODH_{Ms}$. The amino acids conserved among these three species include 9 cysteines, 5

(54) Telser, J.; Benecky, M. J.; Adams, M. W. W.; Mortenson, L. E.; Hoffman, B. M. *J. Biol. Chem.* **1987**, *262*, 6589−6594.

(55) (a) Pollock, R. C.; Lee, H.-I.; Cameron, L. M.; DeRose, V. J.; Hales, B. J.; Orme-Johnson, W. H.; Hoffman, B. M. *J. Am. Chem. Soc.* **1995**, *117*, 8686−8687. (b) Lee, H.-I.; Cameron, L. M.; Hales, B. J.; Hoffman, B. M. *J. Am. Chem. Soc.* **1997**, *119*, 10121−10126.

(56) Trumpower, B. L.; Gennis, R. B. *Annu. Rev. Biochem.* **1994**, 675−716.

(57) Roberts, L. M.; Lindahl, P. A. *J. Am. Chem. Soc.* **1995**, *117*, 2565−2572.

(58) Teixeira, M.; Moura, I.; Xavier, A. V.; Moura, J. J.; LeGall, J.; DerVartanian, D. V.; Peck, H. D., Jr.; Huynh, B. H. *J. Biol. Chem.* **1989**, *264*, 16435−16450.

(59) It is possible that either the histidine (as imidazolate) or the hydroxyl group $-OH_s$ detected in this study forms the bridge between Ni and the Fe_4S_4 center of the C-cluster. Bridging two metals seems less likely for hydroxide that is involved in catalysis as a nucleophile, but it is possible that the status of the bridging ligand changes, for example by CO binding, during catalysis.

(60) Macgregor, S. A.; Lu, Z.; Eisenstein, O.; Crabtree, R. H. *Inorg. Chem.* **1994**, *33*, 3616−18.

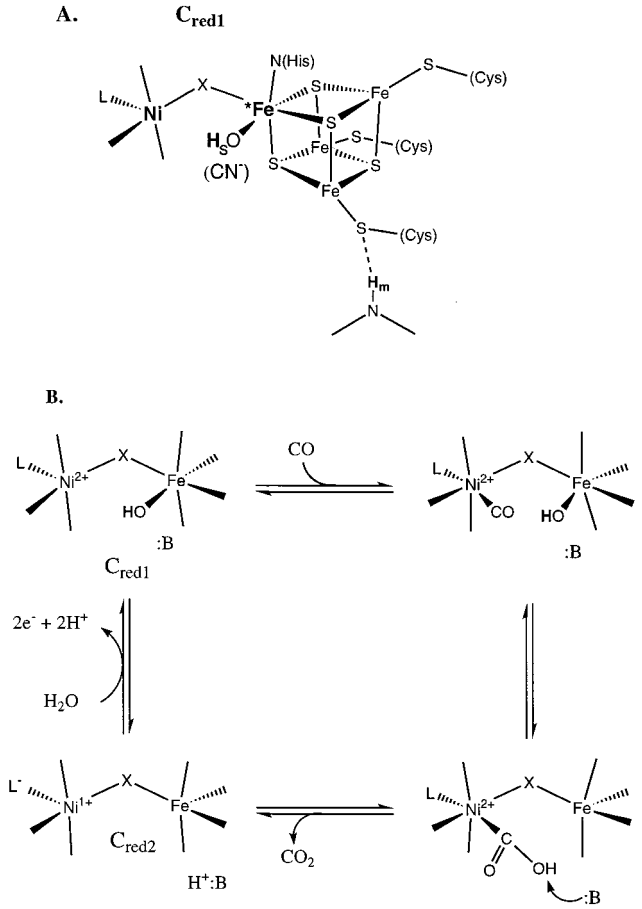

Figure 7. Model of the C-Cluster in $CODH_{Ct}$ and Proposed Mechanism of CO/CO_2 Redox Catalysis. (a) The model of Hu et al. (ref 5) adapted to include the present ENDOR results. In the C_{red1} state, the $[Fe_4S_4]^+$ cluster is proposed to be coordinated by three cysteines, one histidine (coordinated to FCII), and a hydroxide ligand (also coordinated to FCII). It is also possible that either His or hydroxide are the bridging ligand X. The exchangeable protons H_m are shown as due to hydrogen bonding to the cluster. The Ni is trigonal pyramidal and coordinated to ~2 cysteines, ~2 or 3 N/O ligands, an unidentified bridging ligand, and a putative redox-active ligand L. In the C_{red2} state, the hydroxo ligand is absent. (b) The mechanism of Anderson and Lindahl (ref 19) adapted to include the present ENDOR results. The binding of CO to C_{red1} labilizes -OH_s from FCII, similar to the manner in which CO might labilize CN^-. The resulting free -OH_s would be a strong nucleophile that attacks the carbon of CO to afford a carboxylate. The carboxylate is deprotonated by a nearby base, and CO_2 leaves as two electrons reduce the C-cluster to yield C_{red2}. The vertical step on the left-hand side between C_{red1} and C_{red2} is not a single elementary reaction (ref 19).

histidines, 4 aspartates, 3 glutamates, and 2 tyrosines. The B-cluster appears to be a standard $[Fe_4S_4]^{2+/1+}$ cluster,[5] which would implicate 4 cysteine ligands. Since EXAFS of the C-cluster Ni indicates 2 S donors, and there are no conserved methionines in the compared sequences, therefore 2−3 cysteines probably ligate the Ni. Our ENDOR data indicate that the remaining 2−3 cysteines are ligands to the $[Fe_4S_4]$ center. Of the 5 conserved histidine ligands, the ENDOR results show that one probably binds to an iron of the C-cluster. Another histidine (possibly with a pK_a of ~7, see below) might be used in catalysis as a base. All or some of the remaining three histidines may be ligands to the Ni. Thus, we can reasonably account for most of the conserved cysteine and histidine ligands in the sequences of CODH's. Along with the metal content of these species (~ 1 Ni and 8 Fe for $CODH_{Rr}$), this analysis strongly suggests that there are no other metal centers in the subunits of CODH's housing the B- and C-clusters,[61] and no other metal center used in CO/CO_2 redox catalysis.

Implications for the Mechanism of Catalysis. During catalysis, CO probably binds to C_{red1}, is then attacked by OH^-, deposits two electrons into this state (forming C_{red2}), and then leaves as CO_2. In the reverse reaction, CO_2 binds to C_{red2} and is reduced by two electrons, eliminates H_xO, and leaves as CO. The presence of H_s in the C_{red1} state and its absence in C_{red2} is exactly as expected if the hydroxyl substrate for CO/CO_2 redox catalysis is bound to FCII (Fe−OH_s). A mechanism showing this arrangement is presented in Figure 7b.[62]

Our proposal shown in Figure 7, that both CN^- and OH_s bind to FCII and that CO binds to Ni, gives rise to an interesting possibility. It is now fairly well established that CN^- binds to FCII and that the binding of CO (proposed here to occur at the Ni of the C-cluster) reactivates the enzyme by accelerating the dissociation of CN^-.[5,6,63] If CN^- and OH_s both bind to FCII, these results suggest that binding of CO at the Ni center analogously may induce the dissociation of OH_s from FCII during catalysis. This CO-induced dissociation would increase the nucleophilic tendency of ^-OH_s and thus possibly contribute to the observed catalytic properties of the enzyme.

Seravalli et al.[21] reported a small pH-dependent shift in the $g = 2.01$ component of the C_{red1} EPR signal in accordance with a pK_a = 7.2. They suggested that this shift, concurrent with changes in kinetic parameters, reflects the ionization of an enzyme-bound water at the Ni or an Fe of the C-cluster. If H_xO is indeed the substrate, then the lack of changes in the proton ENDOR of samples buffered at pH values spanning this pK_a suggests that the changes in the EPR and kinetic parameters observed by Servalli et al. correspond to the ionization of a species *other* than the substrate H_xO, such as the base denoted B in Figure 7b. Further work is required to settle this issue.

Summary

In this study, we report results of electron nuclear double resonance (ENDOR) spectroscopy of the one-electron reduced (C_{red1}), CN^--inhibited, and CO (or dithionite)-reduced (C_{red2}) forms of the C-cluster from *C. thermoaceticum* CODH. The hyperfine interactions of ^1H, ^{14}N, ^{13}C, and ^{57}Fe observed for

(61) (a) This conclusion is contrary to that of Maupin and Ferry (ref 61b), who recently proposed that the α subunit of CODH from *Methanosarcina thermophila* ($CODH_{Mt}$) (with a molecular mass of 89 kDa and 40% identity with the α subunit of $CODH_{Ms}$ and 67% homology with the β subunit of $CODH_{Ct}$) contained the C-, B-, *and* A-clusters. Although the α subunit of $CODH_{Ct}$ (known to contain the A-cluster) showed only 13% homology with the α subunit of $CODH_{Mt}$, they concluded that each $\alpha\beta\gamma\delta\epsilon$ $CODH_{Mt}$ contains two A-clusters, one in β and a second in α, and that this second site developed through convergent evolution. Since we have accounted for most of the conserved cysteine and histidines in the subunits corresponding to the β subunit of $CODH_{Ct}$, it seems unlikely that a second A-cluster could be in the α subunit of $CODH_{Mt}$. Their conclusion was based on a previous study in which preparations of the isolated $\alpha\epsilon$ dimer (called the Ni/Fe−S component) exhibited the NiFeC EPR signal of CO-reduced A-cluster (ref 61c). However, the quantified NiFeC signal intensity in their samples was only ~$^1/_6$ that exhibited by the intact complex, raising the possibility that their samples contained a small amount of intact complex and that it was this complex that gave rise to the signal. (b) Maupin-Furlow, J. A.; Ferry, J. G. *J. Bacteriol.* **1996**, *178*, 6849−6856. (c) Lu, W.-P.; Jablonski, P. E.; Rasche, M.; Ferry, J. G.; Ragsdale, S. W. *J. Biol. Chem.* **1994**, *269*, 9736−9742.

(62) (a) Further evidence for a bimetallic mechanism for CO/CO_2 redox catalysis comes from a study of a dinuclear palladium complex (ref 62b). Both Pd atoms in the complex appear to cooperate in binding and reducing CO_2: one Pd was proposed to bind the C of CO_2 while the other bound one of the oxygen atoms. This arrangement dramatically enhanced the rate of catalysis relative to the corresponding mononuclear complex. (b) Steffey, B. D.; Curtis, C. J.; DuBois, D. L. *Organometallics* **1995**, *14*, 4937−4943.

(63) Ensign, S. A.; Hyman, M. R.; Ludden, P. W. *Biochemistry* **1989**, *28*, 4973−4979.

the $CODH_{Ct}$ C-cluster support and extend the current Ni−X−$[Fe_4S_4]$ model in which a $[Fe_4S_4]$ center is linked through a unique Fe to a Ni ion. ^{61}Ni ENDOR was not observed, supporting the model that the unpaired electron spin is localized on the $[Fe_4S_4]$ component of the cluster in both the C_{red1} and C_{red2} states. Given this, the hyperfine interactions observed by ENDOR most probably reflect species associated with the $[Fe_4S_4]$ component.

The main observations from this study are the following:

1. A hydroxide or water ligand (H_xO) appears to coordinate FCII of the $[Fe_4S_4]^{1+}$ center of C_{red1}. This ligand is lost upon treatment with CN^- or reduction to the C_{red2} state, and is interpreted to be the substrate in catalysis.

2. Nitrogen ENDOR features are assigned to a histidine ligand to the $[Fe_4S_4]$ center in C_{red1} and C_{red2}.

3. The large maximum Fe hyperfine couplings of $A(^{57}Fe) >$ 40 MHz support the unique nature of the $[Fe_4S_4]^{1+}$ cluster in both the C_{red1} and C_{red2} states.

4. CO or its oxidized products are not bound to the $[Fe_4S_4]$ center in C_{red2}.

Acknowledgment. This work was supported by grants from the National Institutes of Health (GM46441 to P.A.L. and HL13531 to B.M.H.), and the College of Science, Texas A&M University (V.J.D.).

Supporting Information Available: ^{57}Fe ENDOR field-dependent data and assignments of C_{red1} and C_{red2} (5 pages, pring/PDF). See any current masthead page for ordering information and Web access instructions.

JA9731480